Neutron Diffraction by Paramagnetic and Antiferromagnetic Substances

C. G. SHULL, W. A. STRAUSER, AND E. O. WOLLAN
Oak Ridge National Laboratory, Oak Ridge, Tennessee
(Received March 2, 1951)

Neutron scattering and diffraction studies on a series of paramagnetic and antiferromagnetic substances are reported in the present paper. The paramagnetic diffuse scattering predicted by Halpern and Johnson has been studied, resulting in the determination of the magnetic form factor for Mn++ ions. From the form factor, the radial distribution of the electrons in the $3d$-shell of Mn++ has been determined, and this is compared with a theoretical distribution of Dancoff. Antiferromagnetic substances are shown to produce strong, coherent scattering effects in the diffraction pattern. The antiferromagnetic reflections have been used to determine the magnetic structure of the material below the antiferromagnetic Curie temperature. For some substances the magnetic unit cell is found to be larger than the chemical unit cell. The temperature dependence of the antiferromagnetic intensities has been studied, and the directional effects which characterize neutron scattering by aligned atomic moments have been used to determine the moment alignment with respect to crystallographic axes. From studies with magnetic ions possessing both orbital and spin moments, it is found that the antiferromagnetic intensities contain partial orbital moment components along with the spin moment component. The degree of orbital moment contribution agrees satisfactorily with that predicted by models of lattice quenching.

INTRODUCTION

MAGNETIC scattering effects with neutrons were first investigated theoretically by Bloch,[1] Schwinger,[2] and Halpern and co-workers.[3] The early theoretical developments focused upon the interpretation of experiments designed to determine the value of the neutron's magnetic moment through its interaction with the experimentally known and theoretically understood magnetic moments of various atoms and ions in paramagnetic and ferromagnetic substances. Since this time, however, more powerful resonance techniques have been applied which give high precision in the determination of the neutron magnetic moment, and, in consequence, present-day interest in magnetic scattering effects with neutrons has been directed toward a more complete understanding of the basic phenomena which characterize magnetic media.

Early experimentation on neutron scattering by paramagnetic materials was performed by Whitaker and co-workers[4] in a series of transmission and scattering type experiments. Because of the relative weakness and heterogeneous nature of the neutron beams from their Ra-Be source, coupled with the complexity of crystal scattering effects, only general, qualitative conclusions could be drawn from the data. The more recent work at this laboratory[5] and at Columbia University by Ruderman[6] has shown unambiguously the general features of paramagnetic scattering as predicted theoretically by Halpern and Johnson[3] and has yielded information on the nature of the magnetic form factor.

The present paper is concerned with measurements on the scattering or diffraction pattern which is obtained when monochromatic neutrons are incident upon a substance whose atoms possess magnetic moments. Experimental data will be presented for the scattering by various paramagnetic and antiferromagnetic materials, and the interpretation will be given in terms of a magnetic lattice with spin and orbital moment alignment. In a second paper in preparation, we shall extend the discussion to include scattering by magnetized and unmagnetized ferromagnetic materials, treating also some of the neutron polarization phenomena which are associated with ferromagnetic scattering.

SCATTERING OF NEUTRONS BY PARAMAGNETIC SUBSTANCES

The theory of neutron scattering by a true paramagnetic substance has been given in detail by Halpern and Johnson. In such a substance, there exist permanent magnetic moments at individual atomic sites caused by unbalanced electronic moments within the atoms, and these atomic moments are completely uncoupled to each other and directed in random orientation. Because of this randomness the substance will display no permanent macroscopic magnetic moment. Application of an external magnetic field will, however, disturb the randomness and cause partial alignment of the atomic moments, so that an induced macroscopic magnetic moment is evidenced. Thermal disordering effects tend to oppose the alignment caused by the magnetic field, and Langevin showed that the magnetic susceptibility (induced moment per unit field) should vary inversely with absolute temperature, as first determined experimentally by Curie. This can be described by the well-known Curie law,

$$\chi = C_M / T, \qquad (1)$$

where χ is the magnetic susceptibility, T the absolute temperature, and C_M the Curie constant which is

[1] F. Bloch, Phys. Rev. **50**, 259 (1936).
[2] J. S. Schwinger, Phys. Rev. **51**, 544 (1937)
[3] O. Halpern and M. H. Johnson, Phys. Rev. **55**, 898 (1939); O. Halpern and T. Holstein, Phys. Rev. **59**, 960 (1941); Halpern, Hamermesh, and Johnson, Phys. Rev. **59**, 981 (1941).
[4] M. D. Whitaker, Phys. Rev. **52**, 384 (1937); Whitaker, Beyer, and Dunning, Phys. Rev. **54**, 771 (1938); M. D. Whitaker and W. C. Bright, Phys. Rev. **57**, 1076 (1940); **60**, 280 (1941).
[5] C. G. Shull and J. S. Smart, Phys. Rev. **76**, 1256 (1949).
[6] I. W. Ruderman, Phys. Rev. **76**, 1572 (1949).

related to the strength of the individual atomic magnetic moments. Many substances are known to obey this relationship, particularly at high temperatures, but there are frequent departures from the idealized state at low temperatures. In such cases the agreement can be extended in temperature range by the introduction of the Curie-Weiss constant θ into Eq. (1) so that there results the Curie-Weiss law,

$$\chi = C_M/(T-\theta). \quad (2)$$

This modification is considered to be an indication that the magnetic fields of surrounding atoms are interacting to the extent that the magnetic moments are no longer uncoupled, as premised in the development of the simple Curie law. This interaction may become so strong in certain cases that even Eq. (2) fails, and the material may show ferromagnetic or antiferromagnetic behavior.

Since the neutron possesses a magnetic moment, it would be expected to experience a simple dipole-dipole interaction in addition to the usual short-range nuclear interaction upon being scattered by an atom possessing a magnetic moment. Halpern and Johnson have given a convenient formulation of this interaction in terms of differential scattering cross section and scattering amplitude. For the case of complete randomness of atomic dipole orientation, they show that the magnetic scattering is completely *incoherent* and that the scattering by an assemblage of such atoms in a crystal lattice is given by the sum of the scattered intensities from each of the atoms. The differential cross section for magnetic scattering per atom is given by [their Eq. (5.41)]

$$d\sigma_m = \tfrac{2}{3}S(S+1)(e^2\gamma/mc^2)f^2 d\Omega, \quad (3)$$

where S is the spin quantum number of the scattering atom, f is the amplitude form factor, γ is the neutron magnetic moment expressed in nuclear Bohr magnetons, and the other terms have their conventional significance. In contrast to nuclear scattering cross sections which are without a form factor angular dependence (the nuclear size being so much smaller than the neutron wavelength), the magnetic scattering effects are always characterized by their angular dependence, since the electrons which are responsible for the atomic magnetic moment are distributed in a volume whose linear extent is quite comparable to the neutron wavelength ($\sim$1A). The magnetic form factor f will depend upon the radial distribution within the atom of only those electrons which are magnetic donors and in this respect will differ materially from the usual x-ray scattering form factor which is representative of all of the atomic electrons.

The magnetic cross section discussed becomes quite sizeable and even exceeds nuclear cross sections in many cases. An example of this is given in paramagnetic salts containing Mn^{++} ions. This ion is in a spectroscopic S-state, with 5 electrons in the $3d$-shell whose spins are all aligned parallel, so that the spin quantum number of the ion is 5/2. According to Eq. (3), such an

ion should possess a differential magnetic scattering cross section of 1.69 barns/steradian in the forward direction, and this exceeds the coherent nuclear differential scattering cross section for Mn of 0.109 barns/steradian.

With regard to paramagnetic scattering effects, we have investigated the angular dependence of neutron scattering by several Mn^{++} paramagnetic salts, with the idea of establishing quantitative agreement with the theoretical predictions and also of determining experimentally the magnetic form factor. A beam of monochromatic neutrons of wavelength 1.057A was scattered by the sample under study in one of the Oak Ridge neutron diffraction spectrometers. Since the paramagnetic effects appear in the diffuse scattering, it is imperative that the scattering sample be very free of any combined or occluded water, because the very large spin diffuse scattering of hydrogen can easily mask the desired scattering. The hydrogen diffuse scattering, furthermore, possesses an angular variation not unlike the magnetic form factor scattering, thus adding to the difficulties. Very pure and anhydrous samples of MnO, $MnSO_4$, and MnF_2 were prepared by Mr. D. Lavalle of this laboratory for this study, and these were sufficiently anhydrous that the contaminant hydrogen scattering was negligibly small.

The neutron diffraction patterns for all these substances contain various components including (1) nuclear coherent scattering, (2) nuclear spin incoherent scattering, (3) thermal diffuse scattering, (4) multiple scattering in the specimen block, and (5) the paramagnetic diffuse scattering. The first of these is represented by the Debye-Scherrer diffraction peaks, and, since these are localized in angular position in the pattern, there is no difficulty in resolving them from the diffuse scattering. The nuclear spin incoherent scattering arises principally from the Mn scattering, since none of the other nuclei in these compounds exhibits nuclear incoherent scattering,[7] and this should be completely isotropic. By calculation, the spin incoherent scattering is small, and one can reliably make corrections for it. Thermal diffuse scattering is also rather small, vanishingly so for small angles, and can be calculated with the Debye formula making use of experimental data on the elastic constants of the specimen lattice. Among the diffuse scattering contaminants, the largest and most difficult of correction is the multiple scattering in the specimen block. This has been determined in an empirical fashion by studying the diffuse scattering with samples having equivalent scattering and absorption properties but having no magnetic scattering. In general, the total contribution of spin incoherent, thermal diffuse, and multiple scattering for the specimen amounted to about 20 or 30 percent of the total diffuse scattering in the forward direction, so that

---

[7] C. G. Shull and E. O. Wollan, Phys. Rev. **81**, 527 (1951).

the resultant paramagnetic scattering could be evaluated fairly well.

After correcting the diffuse scattering in the diffraction patterns in the aforementioned fashion, the resultant paramagnetic scattering for the three Mn^{++} salts was obtained as shown in Fig. 1. The data are on an absolute scale and are shown as differential scattering cross sections. Because of the relatively large magnetic dilution in $MnSO_4$ as compared to MnF_2 and MnO and the consequent low scattering intensity, the $MnSO_4$ curve is not considered to be as reliable as the other two. The MnF_2 magnetic scattering shows the expected form factor distribution with angle, whereas the MnO curve shows a definite peaking or residual coherence. This suggests that *in MnO at room temperature, the magnetic moments are not completely randomly arranged, but that there exists a short-range magnetic order with neighboring moments tending to be aligned* so that there is partial coherence in the scattering. This is somewhat analogous to the scattering of x-rays by liquids where, because of positional short-range order, residual coherence is obtained in the scattering pattern. In the magnetic short-range order state, the degree of magnetic alignment order is the determining factor rather than the geometrical positional order. Presumably, it will be possible to interpret the magnetic short-range order patterns in terms of short-range order coefficients or parameters just as has been done in the case of chemical short-range order in superlattices.[8] This has not been attempted as yet.

In contrast to the MnO scattering data, that of MnF_2 does not indicate the presence of residual coherence. As a test of this, the pattern was studied when the sample temperature was raised to 400°C, and no significant change in the magnetic pattern was found. Raising the temperature should certainly reduce any short-range magnetic order in the lattice, and the fact that no change was observed indicates that the MnF_2 magnetic pattern corresponds to the true magnetic form factor. According to Eq. (3), the paramagnetic diffuse scattering should amount to 1.69 barns/steradian in the forward direction for Mn^{++}, where $S=5/2$. The extrapolated MnF_2 curve falls perhaps 10 percent lower than the calculated value, and this may be the result of uncertainties in the standardization procedure or in the determination of the angular distribution in the small angle region. The magnetic susceptibility data for Mn^{++} salts are in excellent agreement with calculated values assuming 5 electrons to contribute to the atomic moment, and the above cross section agreement within 10 percent indicates agreement in the number of contributory electron spins to within 5 percent.

RADIAL DISTRIBUTION OF THE ELECTRONS IN THE 3d-SHELL OF Mn^{++}

As mentioned in an earlier section, the magnetic form factor is representative of the spatial distribution

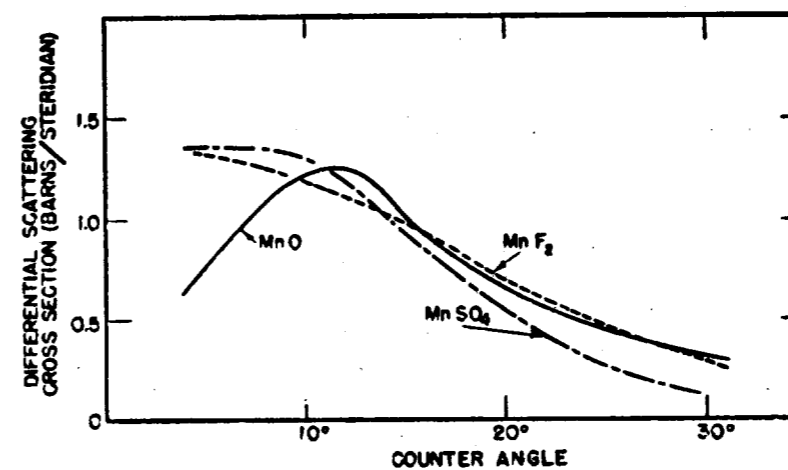[8] J. M. Cowley, J. Appl. Phys. **21**, 24 (1950).

FIG. 1. Paramagnetic diffuse scattering for neutrons by several paramagnetic salts containing Mn^{++} ions.

within the atom of only those electrons which contribute to the atomic magnetic moment—in the case under discussion, the 5 electrons in the 3d-shell. The experimentally determined form factor, which is reproduced in Fig. 2 as the amplitude form factor (along with an estimate of the experimental uncertainty), can be used to obtain the radial distribution curve of the 3d-shell within the atom. For this purpose the usual fourier inversion integral is employed as discussed, for instance, in Compton and Allison.[9] Here

$$u(r) = (2r/\pi) \int_0^\infty kf(k) \sin krdk, \qquad (4)$$

where $u(r)$ is the number of electrons within the shell of thickness dr at radius r, and f is the amplitude form factor in terms of $k = 4\pi(\sin\theta/\lambda)$, with 2θ the scattering angle. This inversion of the experimental form factor has been performed and the resultant radial distribution function $u(r)$ determined as shown in Fig. 3. In order to determine the quantitative significance of $u(r)$, several different experimental form factors were inverted, all
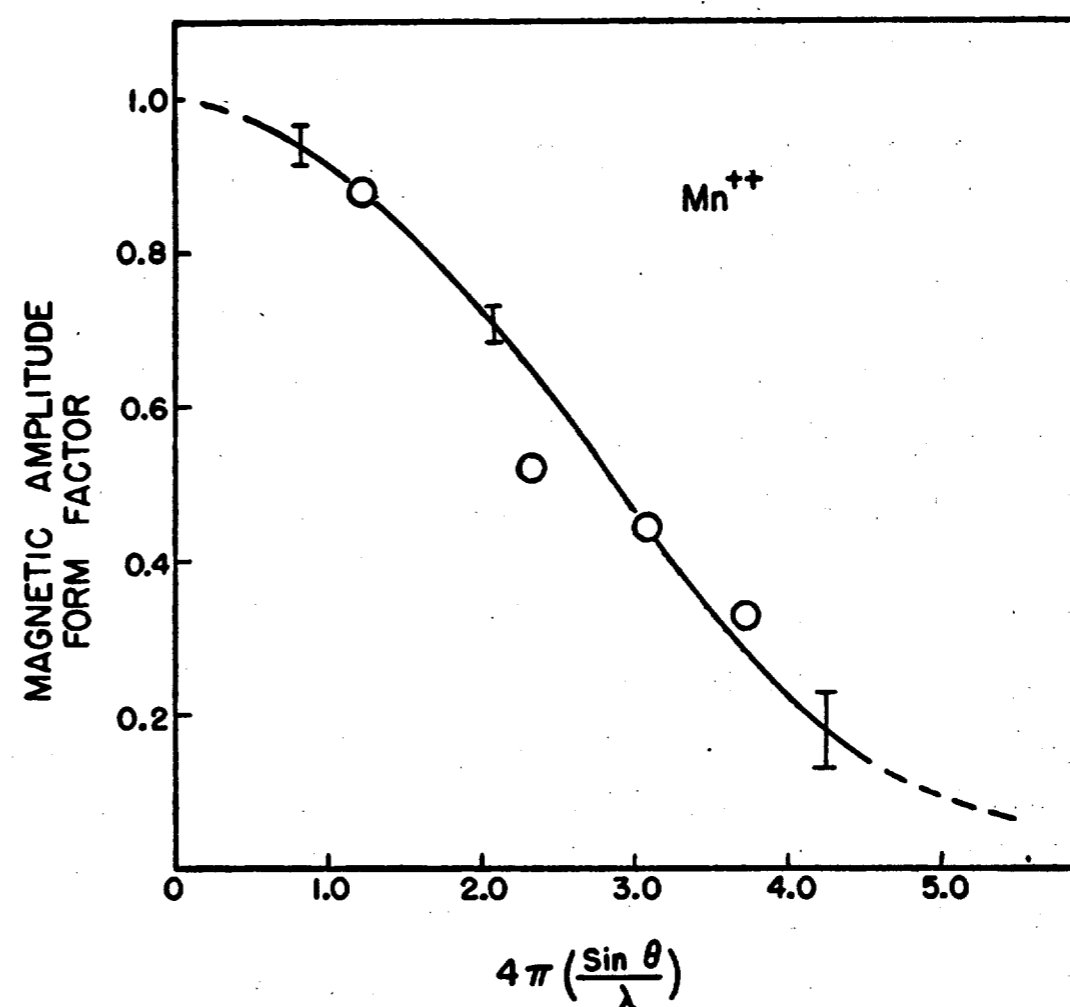

FIG. 2. Magnetic amplitude form factor for Mn^{++} ions. The curve is that obtained from paramagnetic diffuse scattering with estimated error as shown. The points represent values of the form factor obtained from the low temperature antiferromagnetic reflections of MnO.

[9] A. H. Compton and S. K. Allison, *X-rays in Theory and Experiment* (D. Van Nostrand Company, Inc., New York, 1946).
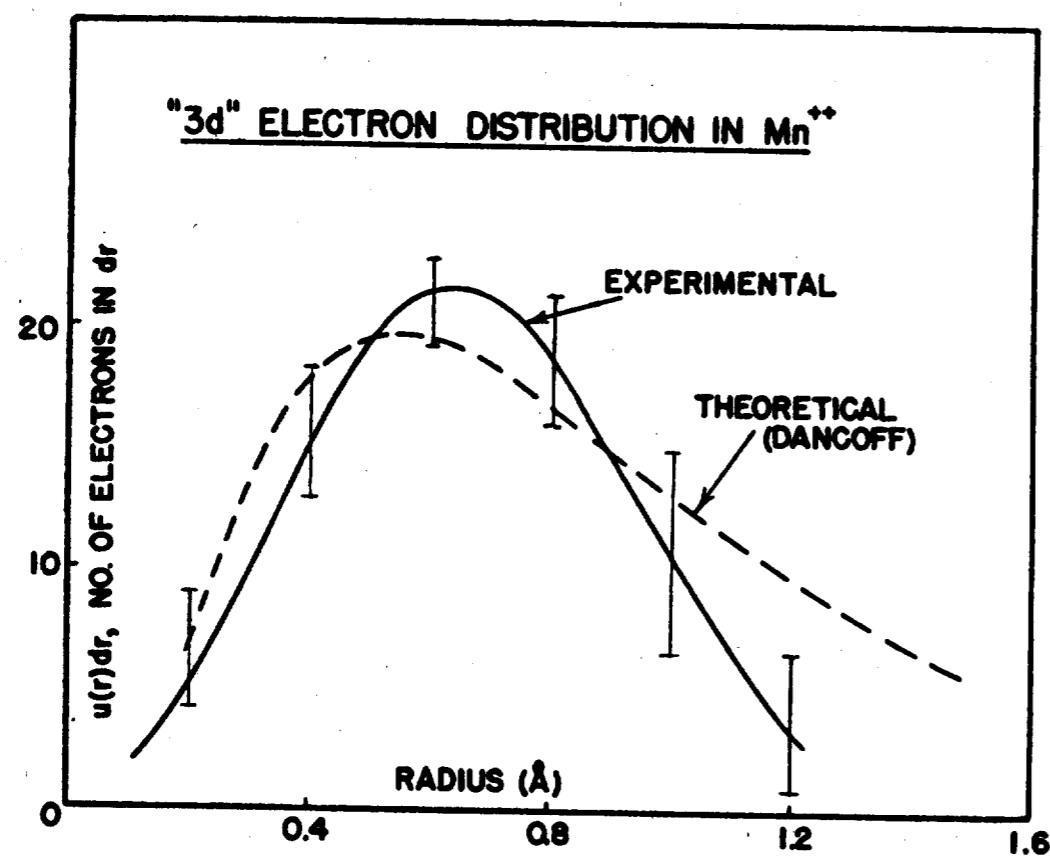
FIG. 3. Comparison between the theoretical distribution of electron radial density in the $3d$-shell of Mn^{++} and that experimentally determined from the magnetic scattering of neutrons. The error representation on the experimental curve is that suggested from inversions performed on several possible experimental form factor curves. The ordinate values are not on an absolute scale.

of which were contained within the suspected uncertainty in the data. The resultant errors in Fig. 3 are a measure of this significance. For comparison purposes a theoretical curve has been calculated for the $3d$-shell in Mn^{++} by Dancoff,[10] using a self-consistent field analysis with exchange effects included. Both the experimental and theoretical curves show maxima in the vicinity of radius 0.6A, but a rather pronounced difference shows up at larger radii values. One possible explanation for this discrepancy might be that the computation was based on an isolated ion, whereas the experimental data were obtained for an ion in a crystal lattice where the distribution might be compressed under the influence of surrounding neighbor ions.

SCATTERING OF NEUTRONS BY ANTI-FERROMAGNETIC SUBSTANCES

Many paramagnetic substances such as MnO and MnF_2 exhibit anomalous magnetic susceptibility and heat capacity behavior at low temperatures. In the former case, for instance, the magnetic susceptibility shows a reversal in its temperature dependence in the vicinity of 120°K. As the temperature is lowered towards 120°K the susceptibility increases according to Eq. (2) with a Curie-Weiss θ of $-510°K$, but in going through 120°K the susceptibility trend reverses itself and decreases as the temperature is further reduced.[11] A marked change in specific heat is also found[12] at this temperature. Early x-ray diffraction studies[12] had shown no change in lattice structure, with the MnO structure being isomorphous with the NaCl face-centered-cubic structure both above and below the

transition temperature.[12a] This anomalous behavior was interpreted as being caused by the development of magnetic order at low temperatures, with an antiferromagnetic lattice existing below the transition temperature or antiferromagnetic Curie point. In such a magnetic lattice some of the neighboring atomic moments are coupled in antiparallel orientation by the quantum mechanical exchange forces. Macroscopically there are as many moments directed in one orientation as in the opposite, so that the susceptibility does not experience large values as in the case of a ferromagnetic lattice below the ferromagnetic Curie point in which the moments are locked in parallel orientation. Theoretical treatment of such antiferromagnetic lattices has been given by Néel,[13] Bitter,[14] Van Vleck,[15] and recently by Anderson[16] and Li.[17]

In this picture it would not be unexpected that a short-range magnetic order could exist in the lattice at temperatures not very elevated with respect to the Curie temperature. The fact that MnO exhibits this property at room temperature, which is some 180° above the Curie temperature of 120°K, shows that the short-range order characteristics can persist over quite a sizeable temperature range. Below the Curie point an entirely different type of magnetic pattern would be expected in the neutron scattering, since the magnetic scattering amplitudes would now show coherent scattering effects. A preliminary report on some of these observations has been given in an earlier letter,[5] and we now discuss in detail these studies.

The theory of neutron scattering by ferromagnetic lattices as developed by Halpern and Johnson[3] can be used in the interpretation of the antiferromagnetic scattering effects. Halpern and Johnson (H-J) show that the differential scattering cross section F^2 per magnetic atom for unpolarized neutron scattering by an oriented magnetic lattice is given as

$$F^2 = C^2 + q^2 D^2, \tag{5}$$

where C is the coherent nuclear scattering amplitude, and D is the magnetic scattering amplitude. The nuclear amplitude cannot be calculated theoretically because of our ignorance of nuclear force fields, but values of C for many nuclei have been determined experimentally.[7] On the other hand, the magnetic interaction can be treated theoretically, and H-J give for D the formulation,

$$D = (e^2/mc^2)\gamma Sf, \tag{6}$$

where the terms have the same significance as for Eq. (3). The absolute sign of the magnetic scattering amplitude D can be either positive or negative, de-

---

[10] Unpublished calculations by S. M. Dancoff.
[11] Bizette, Squire, and Tsai, Compt. rend. **207**, 449 (1938); C. F. Squire, Phys. Rev. **56**, 922 (1939).
[12] B. S. Ellefson and N. W. Taylor, J. Chem. Phys. **2**, 58 (1934). (with references to earlier work by Millar and Anderson).

[12a] See later discussion for more recent x-ray diffraction findings.
[13] L. Néel, Ann. phys. **17**, 64 (1932); **5**, 256 (1936).
[14] F. Bitter, Phys. Rev. **54**, 79 (1938).
[15] J. H. Van Vleck, J. Chem. Phys. **9**, 85 (1941).
[16] P. W. Anderson, Phys. Rev. **79**, 350); Phys. Rev. **79**, 705 (1950).
[17] Yin-Yuan Li, Phys. Rev. **80**, 457 (1950).

pending upon the relative orientations of the atomic and neutron magnetic moments. It is to be emphasized that the square of D in Eq. (5) is a classical or numerical square, in contrast to the quantum mechanical square which appeared in Eq. (3) describing paramagnetic scattering. In oriented magnetic lattice scattering, only a single-spin state is existent, and, hence, the square of the amplitude involves S^2 rather than $S(S+1)$.

The term q^2 in Eq. (5) depends upon the relative orientation of the two unit vectors $\mathbf{e}$ and $\boldsymbol{\kappa}$, where $\mathbf{e}$ is the scattering vector given by

$$\mathbf{e}=(\mathbf{k}-\mathbf{k}')/|\mathbf{k}-\mathbf{k}'|, \qquad (7)$$

where $\mathbf{k}$ and $\mathbf{k}'$ are the incident and scattered wave vectors, and $\boldsymbol{\kappa}$ is a unit vector along the direction of alignment of the atomic magnetic moments. H-J show that

$$\mathbf{q}=\mathbf{e}\times(\mathbf{e}\times\boldsymbol{\kappa}), \qquad (8)$$

so that

$$q^2=1-(\mathbf{e}\cdot\boldsymbol{\kappa})^2. \qquad (9)$$

It is seen that q^2 can attain values between 0 and 1 and, for the particular case where $\boldsymbol{\kappa}$ is randomly directed,

$$q^2 \text{ (random)}=\tfrac{2}{3}.$$

This dependence of q^2 upon the relative directions of scattering and magnetization has been given a direct experimental test in the scattering from magnetized, ferromagnetic substances,[18] and these data show the correctness of the above formulation.

The differential scattering cross section F^2 determines what is available for coherent neutron scattering but tells nothing about the angular distribution of scattered intensity from a magnetic lattice. Details of the scattered intensity in the diffraction pattern will be determined (as in x-ray or electron diffraction) by the crystal structure factors, and from the experimental determination of these factors, one can hope to establish the magnetic lattice. It is interesting to note that according to Eq. (5) there is no coherent interference between the magnetic and nuclear portions of the scattering, and that in essence the two intensities of scattering are merely additive. This is a consequence of the treatment for unpolarized incident neutron radiation and would not be the situation if the neutron magnetic moments were all aligned in the incident beam. For the latter case, the differential scattering cross section contains cross terms between the nuclear and magnetic amplitudes in addition to the above square terms.

MnO

As already mentioned, MnO is thought to be antiferromagnetic below its Curie temperature of 120°K; and Fig. 4 shows neutron powder diffraction patterns taken for this material at 300°K and at 80°K. The pow-

dered sample was contained in a thin walled cylindrical capsule held within a low temperature cryostat. Both patterns were taken of the same sample before and after introduction of liquid nitrogen coolant. The room temperature pattern shows both magnetic diffuse scattering and the Debye-Scherrer diffraction peaks at positions indicated for nuclear scattering. There should be coherent nuclear scattering at both all-odd and all-even reflection positions from this NaCl-type lattice, and since the signs of the nuclear scattering amplitudes are opposite for Mn and for O, the odd reflections, (111) and (311), are strong whereas the even reflections, (200) and (220), are very weak. When the material is cooled to a low temperature, there is no change in the nuclear scattering pattern,[18a] but the magnetic scattering has now become concentrated in Debye-Scherrer peaks at new positions. As can be seen from the figure, these extra magnetic reflections cannot be indexed on the basis of the conventional chemical unit cell of edge length 4.426A. The innermost reflection for this cell is the (100), falling at about $13\tfrac{1}{2}°$ in angle, and there exists a strong magnetic reflection inside of this angle at about $11\tfrac{1}{2}°$. It is possible to index the magnetic reflections, however, on the basis of a cubic unit cell whose axial length is just twice the above, or 8.85A. For this cell the magnetic reflections are all-odd, intensity being observed at the (111), (311), (331), and (511) positions. The $(311)_{mag}$ is on the shoulder of the $(111)_{nucl}$, as can be seen from the asymmetry of this reflection.

This twice-enlarged magnetic unit cell indicates that successive manganese ions along the cube axis directions are oriented differently, so that the repetition distance (for identical scattering power) along the axis is 8.85A
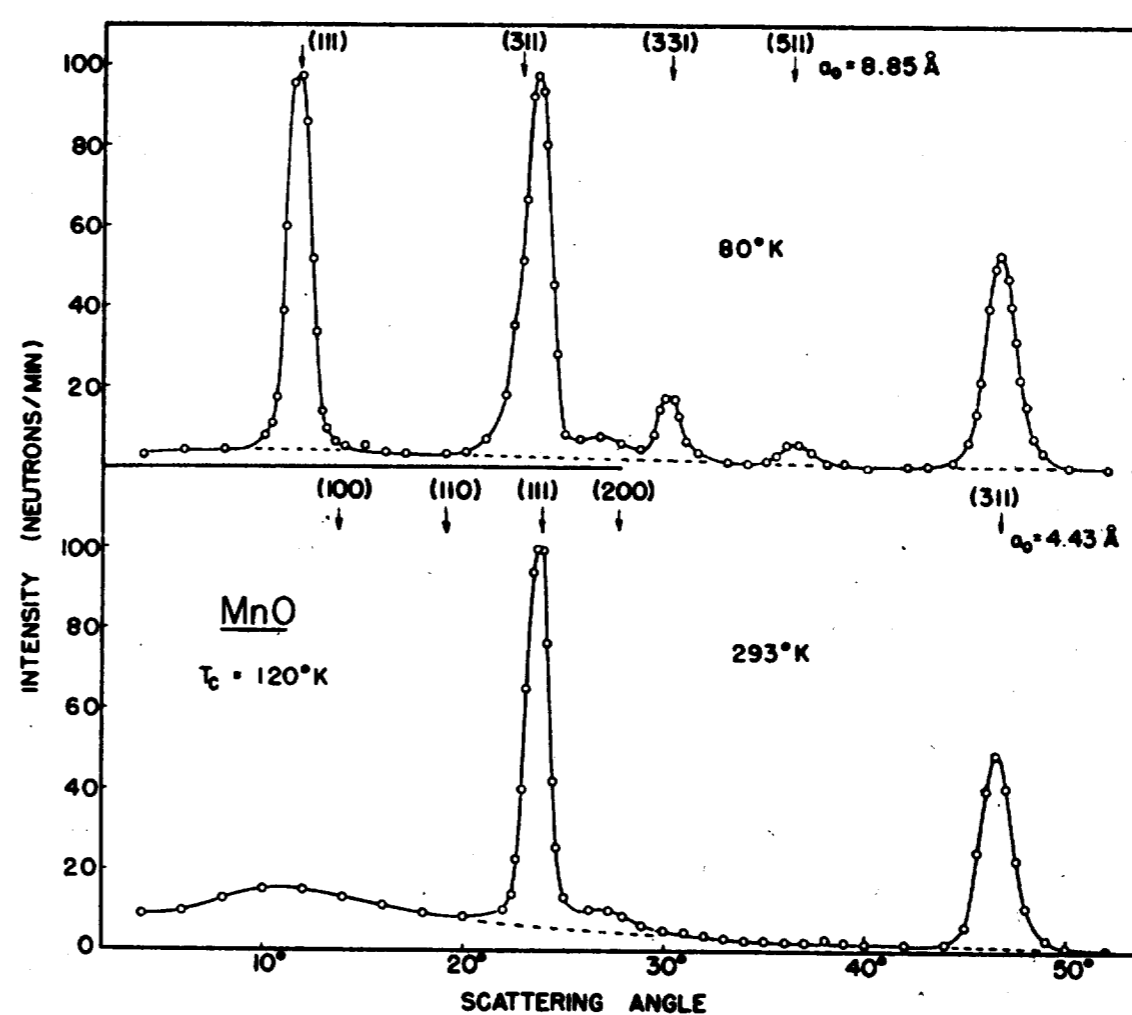

FIG. 4. Neutron diffraction patterns for MnO taken at liquid nitrogen and room temperatures. The patterns have been corrected for the various forms of extraneous, diffuse scattering mentioned in the text. Four extra antiferromagnetic reflections are to be noticed in the low temperature pattern.

[18] Shull, Wollan, and Strauser, Phys. Rev. 81, 483 (1951). See also discussion by D. J. Hughes and M. T. Burgy, Phys. Rev. 81, 498 (1951).

[18a] The nuclear intensities will increase by a few percent due to a slight increase in the Debye-Waller temperature factor.

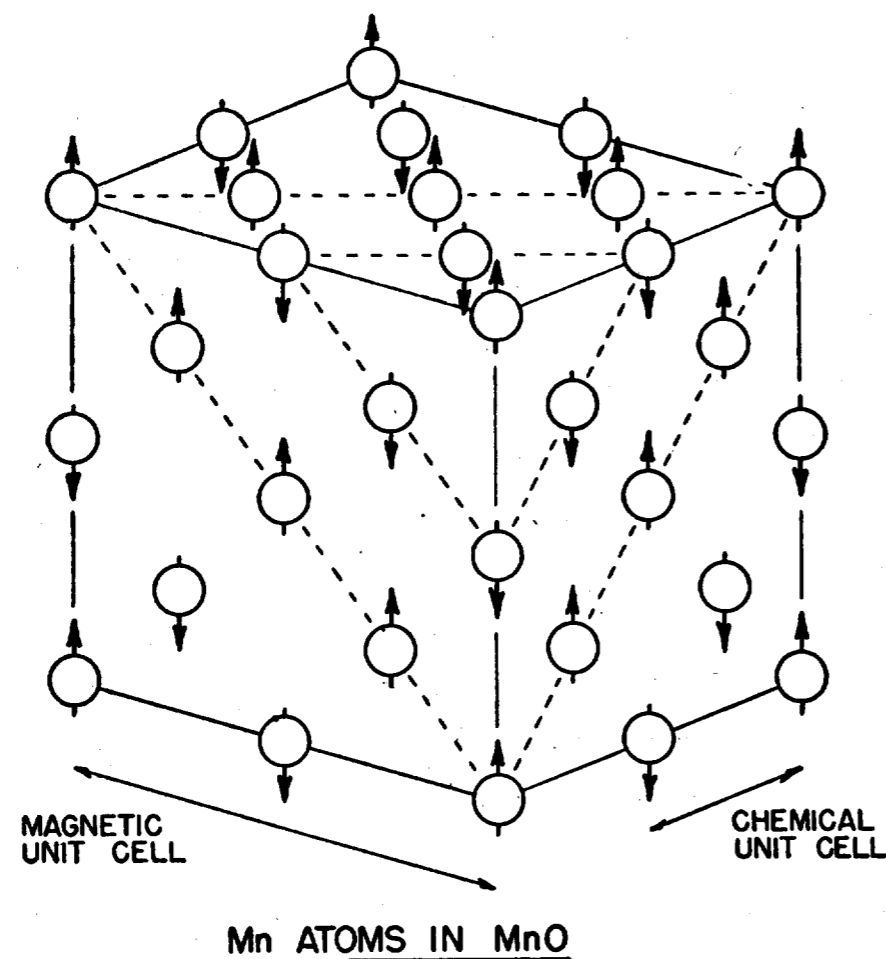MAGNETIC UNIT CELL   CHEMICAL UNIT CELL

Mn ATOMS IN MnO

FIG. 5. Antiferromagnetic structure existing in MnO below its Curie temperature of 120°K. The magnetic unit cell has twice the linear dimensions of the chemical unit cell. Only Mn ions are shown in the diagram.

rather than 4.426A as seen in x-ray scattering or in neutron scattering by the nuclei. The intensities in the magnetic reflections fall off regularly with increasing angle, which is just what the magnetic form factor should require. Because of this weakening of magnetic intensity with increasing angle, only a limited number of magnetic reflections are measurable; in this case the four mentioned above. If nothing were known about the MnO structure, it would be difficult and unconvincing to attempt a magnetic structure determination on the basis of just four intensities. However, x-ray diffraction studies have already shown the positional relationship of the various atoms and the general symmetry of the lattice. Furthermore, the magnetic data and the nature of the quantum mechanical exchange forces responsible for the magnetic alignment limit drastically the number of possible structures which could exist. Néel[19] has suggested several possibilities, and the results of these, along with some others, have been compared with the experimental neutron intensities.

MAGNETIC STRUCTURE OF MnO

Of the various magnetic structure models which were tested, only that shown in Fig. 5 gave satisfactory agree-

ment with the data.[19a] Table I shows the comparison between the experimental intensities and those calculated on the basis of this model. The intensities shown in this table are on an absolute scale and should be compared in absolute as well as in relative values. In the calculated intensities, the magnetic form factor for the 3d-shell in Mn^{++} as determined from the above paramagnetic scattering experiments (see Fig. 2) has been used. Conversely, on the basis of the suggested MnO lattice, the antiferromagnetic reflections can be interpreted in terms of the magnetic form factor, and when this is done, the form factor values shown as discrete points in Fig. 2 are obtained. The intensity agreement shown in Table I appears quite satisfactory, with the exception of the (311) intensity for which the observed value is somewhat lower than the calculated value. As seen in Fig. 4, the (311) magnetic reflection is unresolved from the (111) nuclear reflection, so that its intensity assignment is subject to considerable error, and, thus, the intensity discrepancy may not be significant.

The magnetic lattice is seen to consist of parallel sheets [(111) planes] within which all the Mn ions are coupled ferromagnetically but with antiferromagnetic coupling between neighboring sheets. Of the 12 nearest neighbors surrounding any Mn ion, 6 are oriented parallel to the central ion and 6 are oriented antiparallel. Among the 8 second-nearest neighbors, however, there is complete antiparallel coupling with the central ions. In other words, *along the cube axes there is always antiferromagnetic coupling from one Mn ion to the next, and this coupling persists through, or is caused by, an intermediate oxygen ion between adjacent Mn ions.* This phenomenon of *superexchange*, in which the electronic wave functions of magnetic ions (Mn) overlap those of intermediate ions (O) and thereby result in an exchange coupling of the magnetic ions, was first advanced by Kramers[20] in 1934 and later discussed further by Anderson.[16]

Studies have also been made on MnS and MnSe, which are isomorphous with MnO, above and below their antiferromagnetic Curie temperatures. The patterns obtained were completely similar to those for MnO and hence the magnetic structures are considered to be the same as for the oxide.

In the lattice of Fig. 5 it is to be noticed that not all

TABLE I. Comparison between the observed antiferromagnetic reflection intensities for MnO and those calculated for the magnetic structure model of Fig. 5.

Magnetic reflection	Observed integrated intensity	Calculated intensity (neutrons/min)
(111)	1072	1038
(311)	308	460
(331)	132	129
(511) (333)	70	54

[19] L. Néel, Ann. phys. 3, 137 (1948).

[19a] Reasonable neutron intensity agreement was also found with a random sublattice model, but this type of structure does not correlate with the precision x-ray splitting effects to be discussed later. On this model, the four simple cube sublattices of the face-centered-cubic Mn array are considered to have nearest neighbor antiferromagnetic coupling within a sublattice but with no coupling from one sublattice to another. This model predicts neutron scattering intensities in satisfactory agreement with observation, but then no distortion of the cubic symmetry would be expected below the Curie temperature, whereas this is always found. The model shown in Fig. 5 is identical to the random sublattice model with respect to antiferromagnetic coupling and differs from the latter only in having the various sublattices coupled together in a definite fashion.

[20] H. A. Kramers, Physica 1, 182 (1934).

of the space-diagonal planes ((111) and permutations) are equivalent. This results in a reduced multiplicity, so that instead of eight equivalent (111) planes there result only two which contribute magnetic intensity at the (111) reflection position. The same situation holds for the other magnetic reflections, there being a fourfold reduction in multiplicity or scattered intensity for each.

DETERMINATION OF MAGNETIC MOMENT DIRECTION IN LATTICE

It has been mentioned that the magnetic scattering cross section, and hence the scattered intensity, is dependent upon the relative directions of the ionic magnetic moment and the scattering vector. This dependence has been shown in Eqs. (5) and (9). Since the neutron diffraction data are obtained by scanning across a limited region of the Debye-Scherrer ring, for which the scattering vector is parallel to the normal to the diffracting planes of the particular crystallites in the powder sample which happen to be correctly aligned, one can hope to get information about the orientation of the magnetic moments with respect to the diffracting planes.

For the magnetic lattice of MnO shown in Fig. 5 there appear three cases of interest concerning the relative orientation of the moments and the lattice axes, and the observed scattering intensities should serve to distinguish between these.

(a) The magnetic moments are aligned along arbitrary [100] directions, in other words, along the cube axes, as illustrated in Fig. 5. For this case it can be shown that q^2 (average) = $\frac{2}{3}$ for each of the four observed magnetic reflections in MnO.

(b) The magnetic moments are aligned perpendicular to the ferromagnetic (111) sheets. For this case, q^2 vanishes for the (111) reflection and becomes 32/33 for the (311) and 32/57 for the (331) reflections.

(c) The magnetic moments are aligned arbitrarily in the ferromagnetic (111) sheets. Here q^2 should be 1 for the (111) reflection and various odd values for the other reflections, depending upon the assignment of moment orientation within the sheet.

Table II summarizes the calculated magnetic intensities for each of these three cases, for comparison with the experimentally observed intensities. The (111) intensity is quite sensitive to this selection, and it is seen that case (a) is to be preferred. The data thus suggest that *the moments are aligned along the cube axes either perpendicular to or parallel to the direction of antiferromagnetic coupling.* Since the theory of exchange coupling does not correlate the alignment direction with respect to the relative positions of the magnetic ions, the above directional indication must be representative of some second-order lattice symmetry effect.

It is to be emphasized that the aforementioned conclusions are derivable from random powder samples without the necessity of single-crystal or single-domain study. Only those crystallites in the powder which happen to be oriented with the normal to the Bragg reflecting planes parallel to the scattering vector will contribute intensity to that portion of the Debye-

TABLE II. Comparison between observed MnO antiferromagnetic intensities and those calculated for various models of magnetic orientation with respect to crystallographic axes.

| | Calculated for various oriented models | | | Observed (neutrons/min) |
	(a)	(b)	(c)	
(111)	1038	0	1560	1072
(311)	460	675	...	308
(331)	129	109	...	132
(511) (333)	54	24	...	70

Scherrer ring under study. The orientation of the magnetic moments relative to this normal will affect the observed magnetic intensity. All of the other crystallites which are not correctly aligned in the above sense contribute no intensity and, hence, are not being viewed in the observation.

DEPARTURE FROM CUBIC SYMMETRY IN MnO

At room temperature, precison x-ray diffraction studies on MnO have shown it to be strictly cubic in symmetry. Recently, however, Tombs and Rooksby[21] have shown that, at low temperatures in the vicinity of liquid nitrogen temperature, the x-ray lines are split slightly so that the true symmetry becomes slightly rhombohedral. This implies that the various (111) distances within the unit cell become slightly different at low temperatures. The magnetic structure model of Fig. 5 is very suggestive of this type of splitting, since, indeed, the lattice forces in the various (111) directions would be expected to differ somewhat.

Other oxides such as NiO, FeO, and CoO have been studied, also by Tombs and Rooksby, at various temperatures, and here again lattice splitting effects are found. These oxides all become antiferromagnetic at
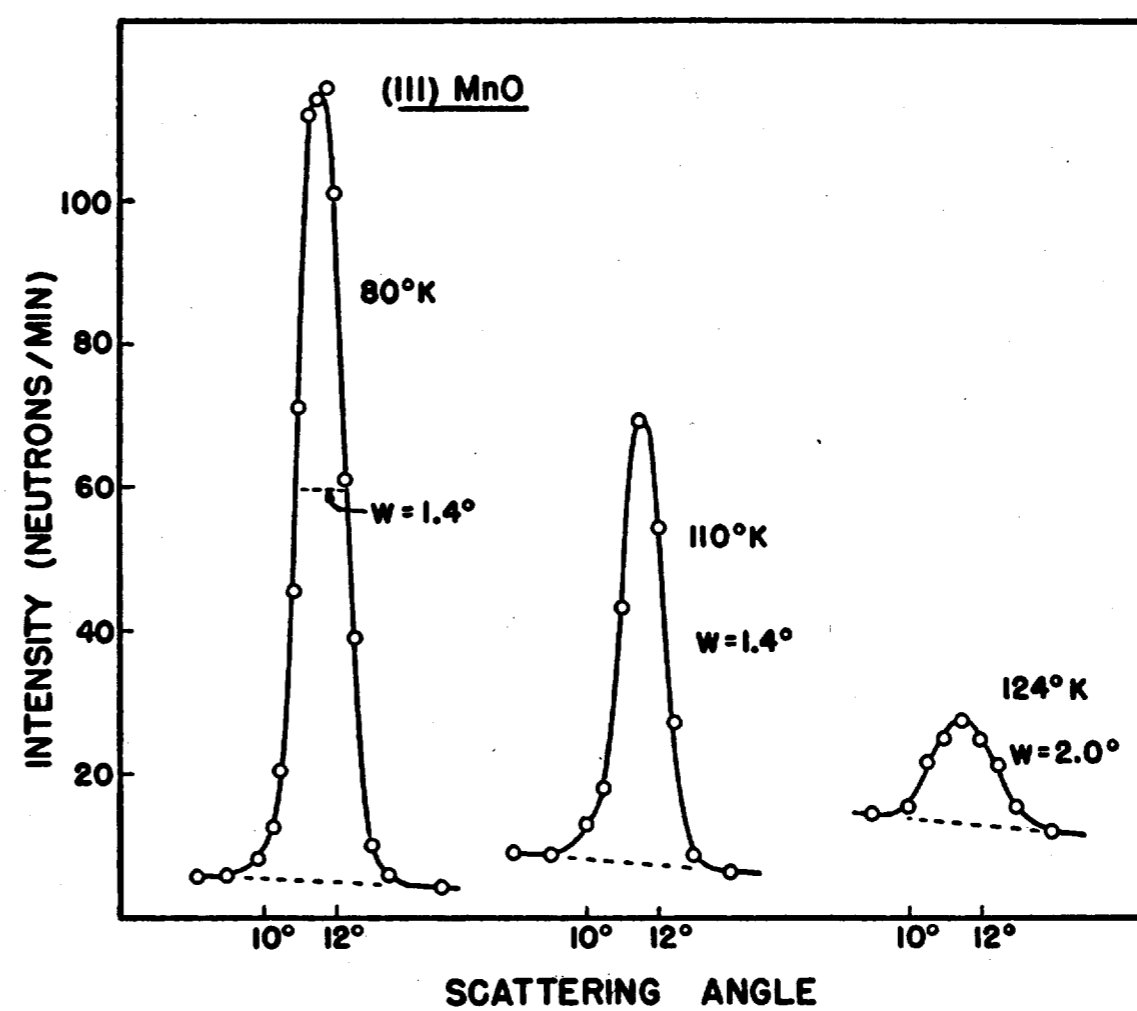

FIG. 6. The (111) antiferromagnetic reflection of MnO as obtained at various temperatures. A noticeable broadening occurs in the vicinity of the Curie temperature.

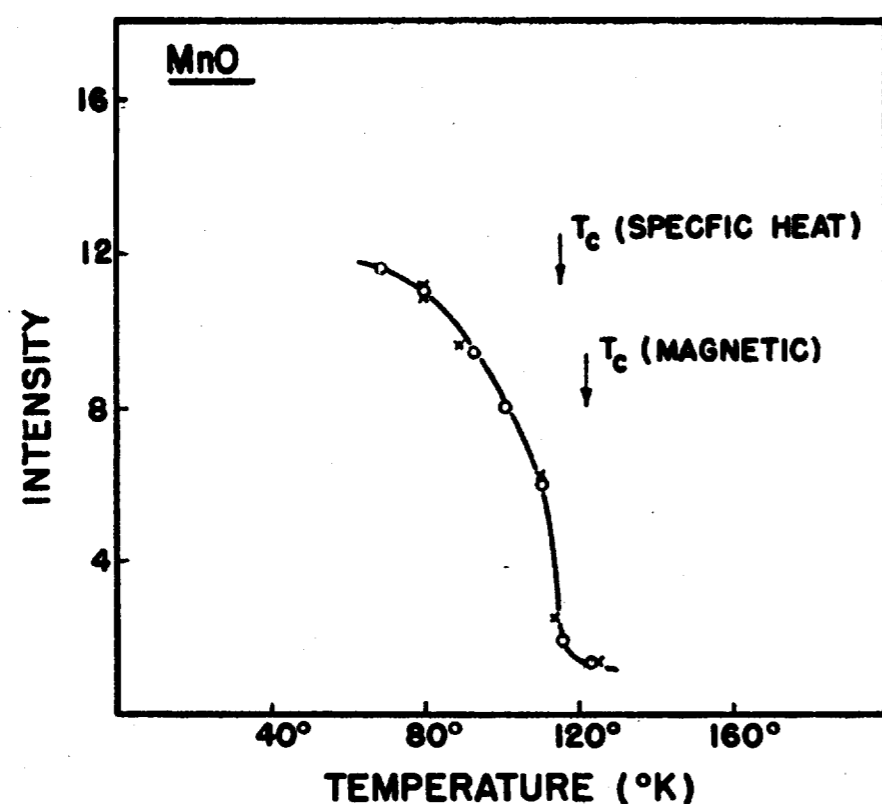[21] N. C. Tombs and H. P. Rooksby, Nature 165, 442 (1950).

FIG. 7. Temperature dependence of magnetic intensity for MnO. The Curie temperatures suggested by specific heat and magnetic susceptibility data are shown.

suitably low temperatures, and undoubtedly the lattice splitting effects are to be associated with the appearance of an antiferromagnetic lattice. This has been discussed recently by Greenwald and Smart.[22]

TEMPERATURE DEPENDENCE OF THE MAGNETIC INTENSITIES

A study has been made of the intensity in the antiferromagnetic pattern at and below the antiferromagnetic Curie temperature. The (111) magnetic reflection in MnO was scanned, with the specimen held at various temperatures. Typical diffraction peaks are shown in Fig. 6, and the data are summarized in Fig. 7. A sharp increase is seen to occur as the temperature is lowered through 120°K, followed by a more gradual approach to a saturation intensity. The Curie temperatures suggested by magnetic susceptibility and specific heat data are also shown in the figure. The temperature dependence of scattered intensity suggests that the magnetic lattice perfection improves as the temperature is reduced, with fewer and fewer local mistakes or faults in alignment appearing. In the peak for 124°K in Fig. 6 there is some evidence of line broadening, and a simple calculation of magnetic crystallite size which would account for this broadening yields the value 50A.

In the comparison of the various structural models with experiment it is necessary to use experimental intensities for the well-ordered lattice. From the intensity dependence shown in Fig. 7, the saturation intensities at 0°K were estimated, and these are the intensities shown in Tables I and II.

OTHER CUBIC OXIDES

All the data so far presented have been for materials containing Mn^{++} ions. This ion is in a normal $^6S_{5/2}$ state according to spectroscopic data, and, therefore, its magnetic moment should have only electron spin contributions with no angular momentum component. As mentioned earlier, the magnetic suscepti-

bility data taken for a variety of Mn^{++} salts support the contention that the ionic moment is equal to that of the 5 electronic spin moments in the $3d$-shell with no orbital moment contribution.

In addition to MnO, scattering data on other isomorphous oxides of the transition elements, FeO, CoO and NiO, have been obtained above and below their antiferromagnetic Curie temperatures. All of these oxides show susceptibility and specific heat anomalies similar to those of MnO but at different temperatures. Data for these oxides are of interest because the various magnetic ions possess orbital momentum components as well as spin components in contrast to the above considered Mn^{++} compounds. Since there is a magnetic moment associated with the orbital momentum values, it might be expected that this, as well as the usual electron spin moment, would contribute to the scattered neutron intensity.

Figures 8, 9, and 10 show the neutron diffraction patterns for FeO and CoO at liquid nitrogen temperature and at room temperature and for NiO at room temperature. In the latter case,[22a] the antiferromagnetic Curie temperature of 250°C is well above room temperature, so that it is unnecessary to cool the substance to invoke the rigid magnetic lattice. *The antiferromagnetic patterns for all of these cubic oxides show the characteristic double-size magnetic cell with reflections being observable at only all-odd indexed positions.* All of the magnetic reflections show the characteristic form factor decline of intensity with increasing angle of scattering. There are, of course, pronounced differences in both nuclear and magnetic intensity for the different sub-
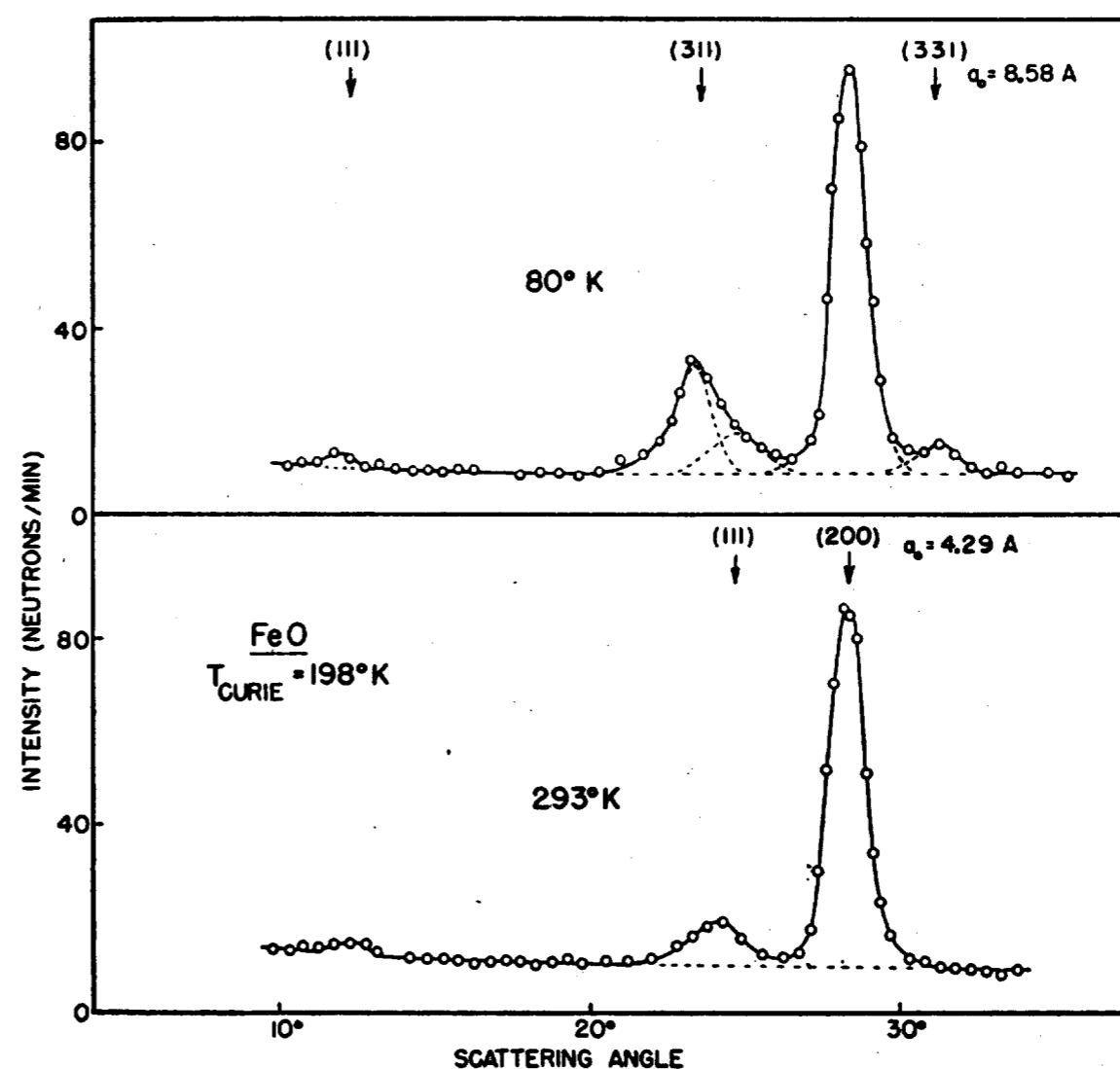

FIG. 8. Neutron diffraction patterns for FeO taken at liquid nitrogen and room temperatures.

[22] S. Greenwald and J. S. Smart, Nature 166, 523 (1950).

[22a] Various samples of NiO enriched in the nickel isotopes Ni^{58}, Ni^{60}, and Ni^{62} have also been examined, and, although the nuclear reflections show pronounced differences from sample to sample, the antiferromagnetic reflections are similar in intensity.

stances, since the nuclear scattering amplitudes and the ionic magnetic moments differ widely.

The intensities and reflection positions in all of the patterns are consistent with a common structural model of the type shown in Fig. 5 for MnO, but with some differences in detail, such as in absolute orientation of the magnetic moments in the lattice and in the strength of the magnetic moments. These differences can be seen most easily when the powder intensities are converted to differential scattering cross sections per magnetic ion for all of the magnetic reflections. This conversion puts the data on an absolute scale and eliminates all of the instrumental and lattice characteristics such as multiplicity, angle of scattering, sample density, etc. A direct comparison is then possible with the various theoretical predictions of the magnetic cross section, depending upon the type of spin and angular momentum coupling in the ion or the degree of orbital momentum quenching in the lattice. The differential scattering cross sections obtained from the experimental data are summarized in the points of Fig. 11 for each of the four simple oxides under discussion. The curves shown in the figure are various theoretical curves; discussion of them will be given later.

All of the experimental points in this figure show the expected form factor variation with angle, with the single exception of the value characteristic of the innermost (111) magnetic reflection of FeO. This particular reflection is very weak or even absent for FeO (see diffraction pattern), whereas the outer FeO reflections appear normal in intensity and form factor behavior. A possible explanation for this follows from the directional effect considerations given in the MnO section. There it was shown that the magnetic moment alignment in MnO was indicated as being along the cube

FIG. 10. Neutron diffraction pattern for NiO taken at room temperature. The Curie temperature is well above room temperature, so the antiferromagnetic reflections appear here.

axis, i.e., case (a) was considered to be correct. However, if the magnetic moments in FeO are aligned perpendicular to the ferromagnetic sheets of the latter [case (b)], then no intensity would be expected in the (111) magnetic reflection, whereas the other (311) and (331) reflections would possess normal intensity. This situation could, then, account for the observations on FeO. Similar arguments for the CoO and NiO data suggest that these are similar to MnO with respect to moment alignment.

In order to compare the observed magnetic scattering data with the theory, we note that Halpern and Johnson considered, for convenience, only the case where the ionic moment was due to spin only. The generalization to cases where the magnetic moment is due to combined spin and orbital angular momentum is formally straightforward; however, we shall discuss it only briefly.[22b] For the general case we note two important differences from the spin-only case:

1. The contribution of the orbital moment to the ionic moment will depend among other things upon the type of coupling in the atom, the symmetry of the crystalline field ("quenching"), and the exchange coupling in the lattice (e.g., ferromagnetism or antiferromagnetism). This will be discussed only for the particular cases at hand.

2. The form factor to be expected in a case where $L \neq 0$ will, in general, be a function not only of $(\sin\theta/\lambda)$ but also of the orientation of the asymmetric ion with respect to the particular scattering planes. For small $(\sin\theta/\lambda)$, this deviation from the form factor characteristic of spherical symmetry is small, but is not necessarily small for larger $(\sin\theta/\lambda)$. In the following we shall assume the Mn^{++} form factor (already discussed) for all cases, neglecting the deviations from spherical symmetry as well as the changes expected from different values of Z. This procedure, though justifiable only as a first orientation, is in reasonable agreement with the experimental data.

In the following we shall, furthermore, assume that (a) Russell-Saunders coupling holds in all cases, (b) the crystalline fields are stronger than the $L \cdot S$ coupling but weaker than the interaction leading to Russell-Saunders coupling so that the orbital angular mo-
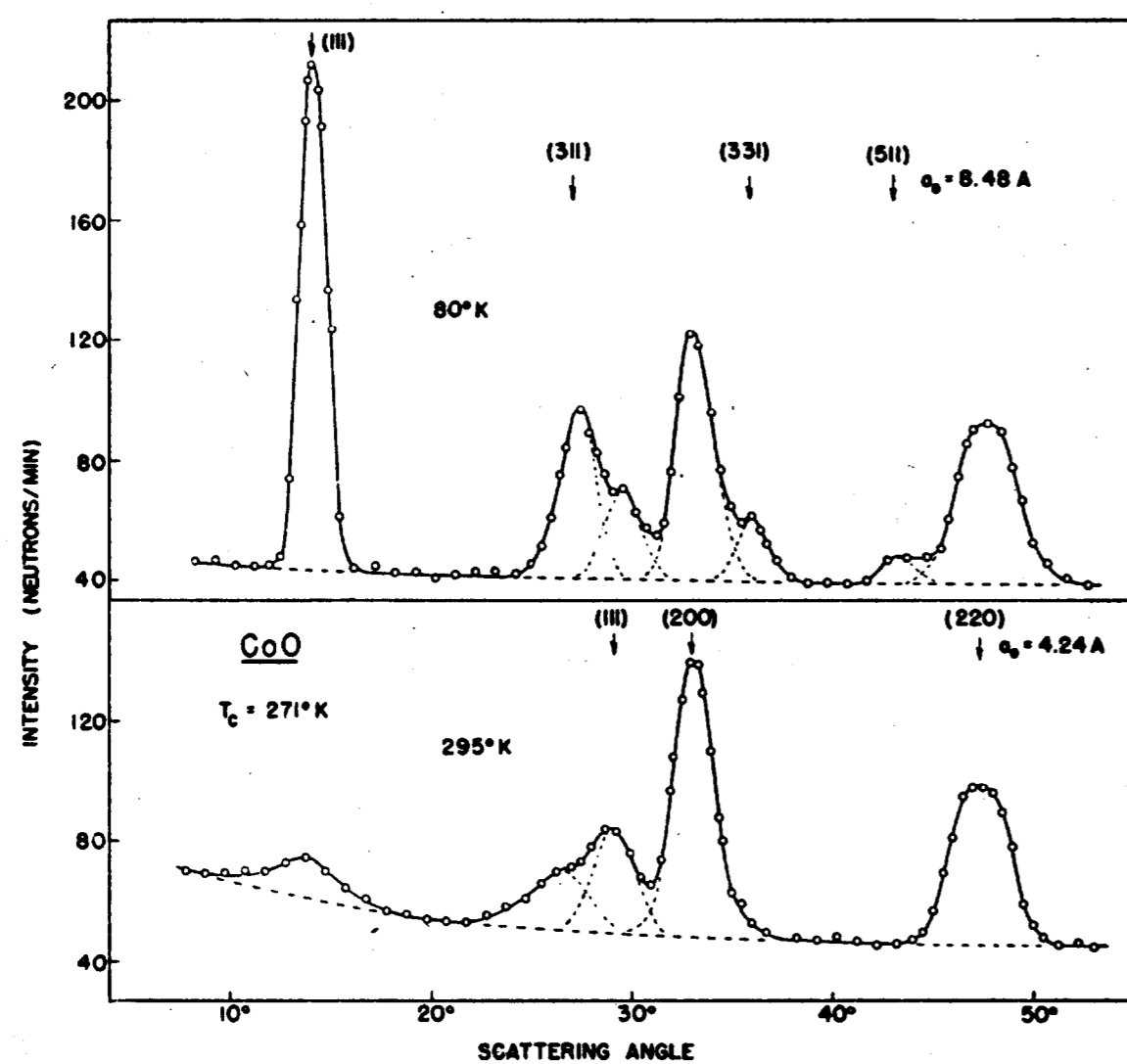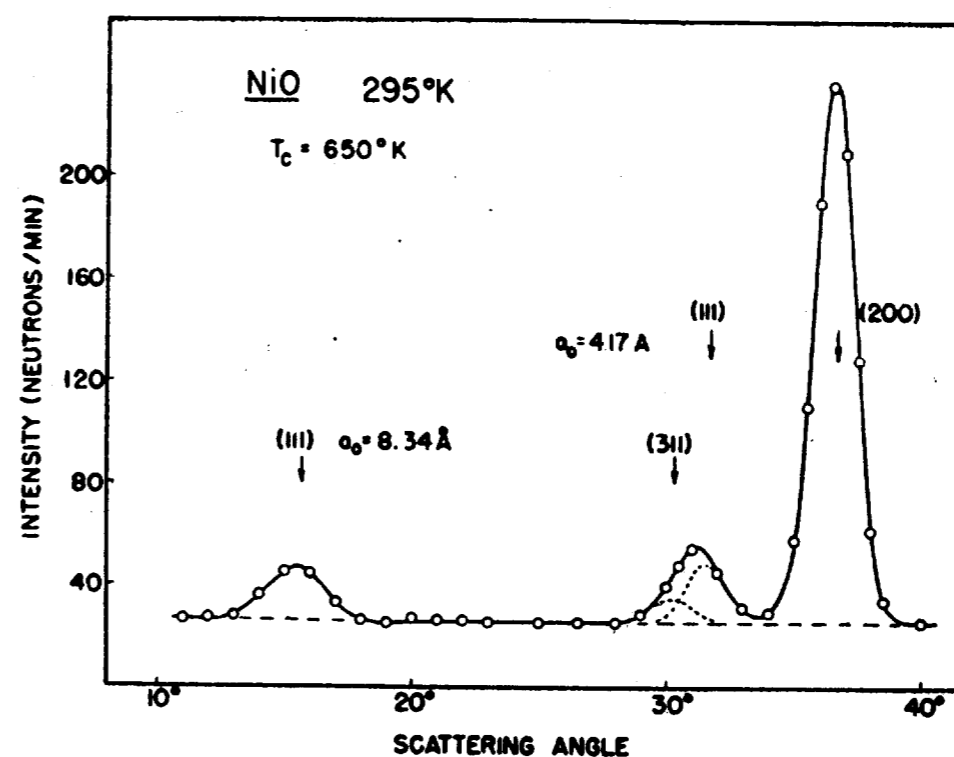

FIG. 9. Neutron diffraction patterns for CoO taken at liquid nitrogen and room temperatures. There is still remnant antiferromagnetic intensity at room temperature, which disappears as the temperature is increased.
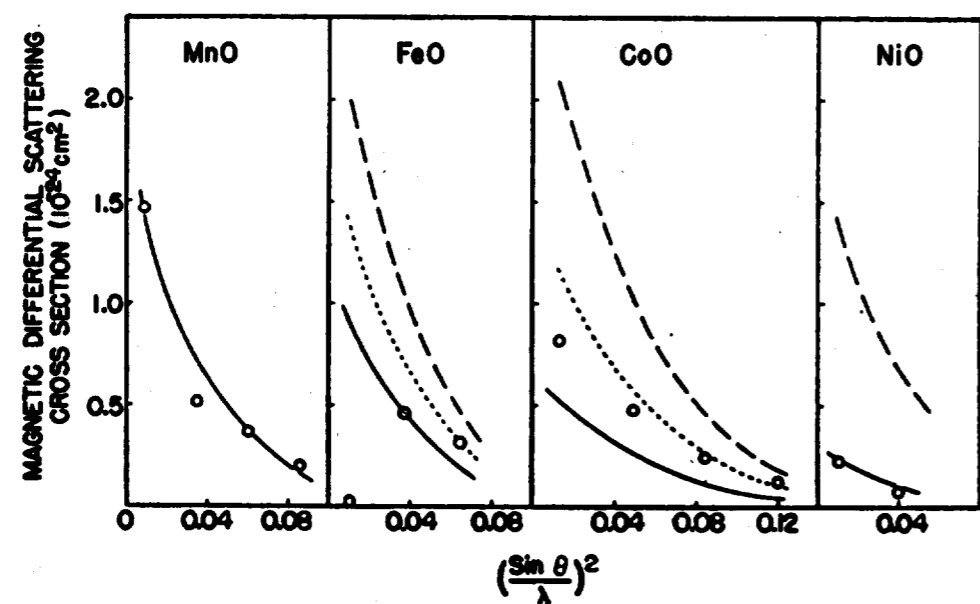
FIG. 11. Representation of the magnetic differential scattering cross sections corresponding to the various antiferromagnetic reflections of MnO, FeO, CoO, and NiO. The points are from experimental data; the solid line corresponds to that calculated for spin-only scattering with complete quenching of orbital moments, the dashed line corresponds to that calculated for the free ion in which the spin and orbital moments add, and the dotted line corresponds to that calculated for the level splitting in the crystalline field. All of the curves are calculated with the Mn^{++} form factor and represent a first approximation to that which is correct for the other ions.

mentum is quenched to some degree, and (c) antiferromagnetic coupling leads to a definite spatial orientation of the spin moment for a given atom in the lattice. The simplest case is that of Mn^{++}, where the free ion is in the spectroscopic state $^6S_{5/2}$ and therefore displays none of the difficulties mentioned above. Co^{++} and Ni^{++} are in F-states ($L=3$) in the free ion ($^4F_{9/2}$ and $^3F_4$, respectively), and according to Bethe[23] an F-level splits in a cubic field into three levels, two triply degenerate levels (magnetic) and one nonmagnetic single level. Van Vleck[24] and Schlapp and Penney[25] have assigned the single level in Ni^{++} to be the lowest lying and normally occupied level, and hence, we expect Ni^{++}, like Mn^{++}, to show a spin-only magnetic moment. In other words, the crystalline field has completely quenched[25a] the orbital contribution to the magnetic moment. (Although Ni^{++} has a spin-only moment, it is to be noted that the form factor for scattering may still display spatial orientation effects.) As its lowest level Co^{++} has one of the triply degenerate magnetic levels, and therefore, a partial quenching of the orbital moment is to be expected. Similarly Fe^{++}, $^5D_4$ for the free ion, has the D-state split by the cubic field into two levels, one triply degenerate and one doubly degenerate, with the latter nonmagnetic. Again Van Vleck[24] assigns the triply degenerate level as the normal one in Fe^{++}, and partial quenching is to be expected.

To calculate the expected magnetic moment, we use the fact that the spins are oriented in the antiferromagnetic lattice and this, by virtue of the **L·S** force, orients the remaining orbital moment. Since the **L·S**

[23] H. Bethe, Ann. Physik **3**, 133 (1929).
[24] J. H. Van Vleck, Phys. Rev. **41**, 208 (1932).
[25] R. Schlapp and W. G. Penney, Phys. Rev. **42**, 666 (1932).
[25a] This picture is some what oversimplified for the Ni^{++} ion since recent experiments (see discussion by C. Kittel, Phys. Rev. **76**, 743 (1949)) do suggest some orbital contribution in this ion. This is not pronounced, however, and, since the magnetic scattering intensities are so low for this ion, the simple theory was considered adequate in initial interpretation.

coupling aligned the moments parallel for the free ion; the spin and orbital moments are taken to add together in the crystalline lattice case. For a cubic field the orientation of the spin moment is unimportant to the degree of quenching, and the effective magnetic moment for both Fe^{++} and Co^{++} turns out to be just $(2S+\frac{1}{2}L)$.

The magnetic moments predicted from the level assignments cited [$2S$ for Mn^{++} and Ni^{++}, $(2S+\frac{1}{2}L)$ for Fe^{++} and Co^{++}] have been used along with the Mn^{++} form factor to give the theoretical curves for the magnetic scattering cross section shown in Fig. 11. For comparison, there is also shown in the figure (a) the curve (Solid line) for complete quenching, with the magnetic moment corresponding to $2S$ and (b) the curve (dashed line) for the free ion, with the moment corresponding to $(2S+L)$. It is to be seen that the data for Mn^{++} and Ni^{++} are in good agreement with the expected spin-only curves. This also indicates that the approximation of all of the form factors by the Mn^{++} form factor is not grossly in error. For Co^{++}, and to a lesser extent for Fe^{++}, the experimental data are in reasonable agreement with the theoretical curves based on partial quenching. It is to be noted again that the very low value for the innermost (111) FeO reflection is the result of a different effect, namely, that q^2 vanishes for this reflection as already discussed. In view of the approximations involved, the general agreement of the observed intensities or cross sections with those expected appears satisfactory.

The aforementioned quenching effects in Fe^{++}, Co^{++}, and Ni^{++} compounds appear also in the paramagnetic susceptibility and gyromagnetic ratio measurements, and, in fact, the early theory was directed towards an understanding of these observations. The
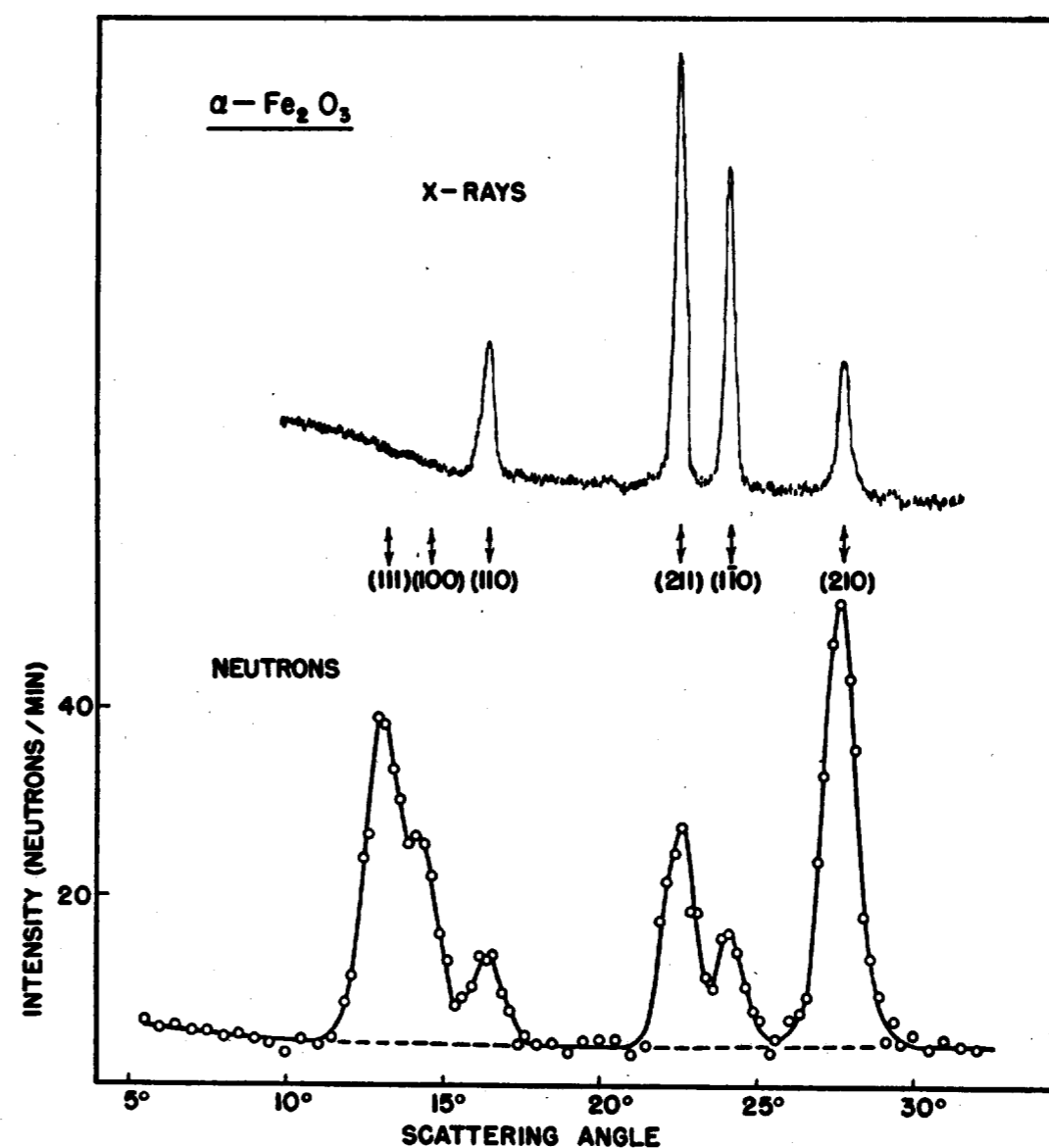

FIG. 12. Comparison of x-ray and neutron diffraction patterns for α-Fe$_2$O$_3$ hematite. The innermost two reflections are antiferromagnetic in origin and are absent in the x-ray case.

effective magnetic moments for these ions as calculated from the paramagnetic susceptibility show departures from spin-only values in the fashion described for crystalline field level splitting, as do also the g-factors. This is summarized in several tables of Van Vleck[26] and of Stoner.[27]

As mentioned, Tombs and Rooksby[21] have shown for all of these simple cubic oxides at temperatures below their antiferromegnetic Curie points a slight departure from cubic symmetry. Their precision x-ray studies have suggested (a) a rhombohedral unit cell with enclosed angle slightly larger than 60° (if strictly cubic, the equivalent angle would be exactly 60°) for MnO and NiO, (b) a rhombohedral cell with an angle slightly smaller than 60° for FeO, and (c) a tetragonal unit cell with axial ratio about 0.995 for CoO. Here again the neutron scattering similarity from oxide to oxide shows the same grouping as does the x-ray line splitting. With respect to moment alignment in the unit cell MnO and NiO show the same behavior with no crystalline field orbital momentum effects with respect to moment alignment. FeO behaves differently, and the CoO scattering data indicate a considerable coupling of the orbital momentum to the spin momentum. No detailed picture of the correlation between the scattering data and the splitting observations are available as yet, but it may be that a detailed investigation will show such a correlation.
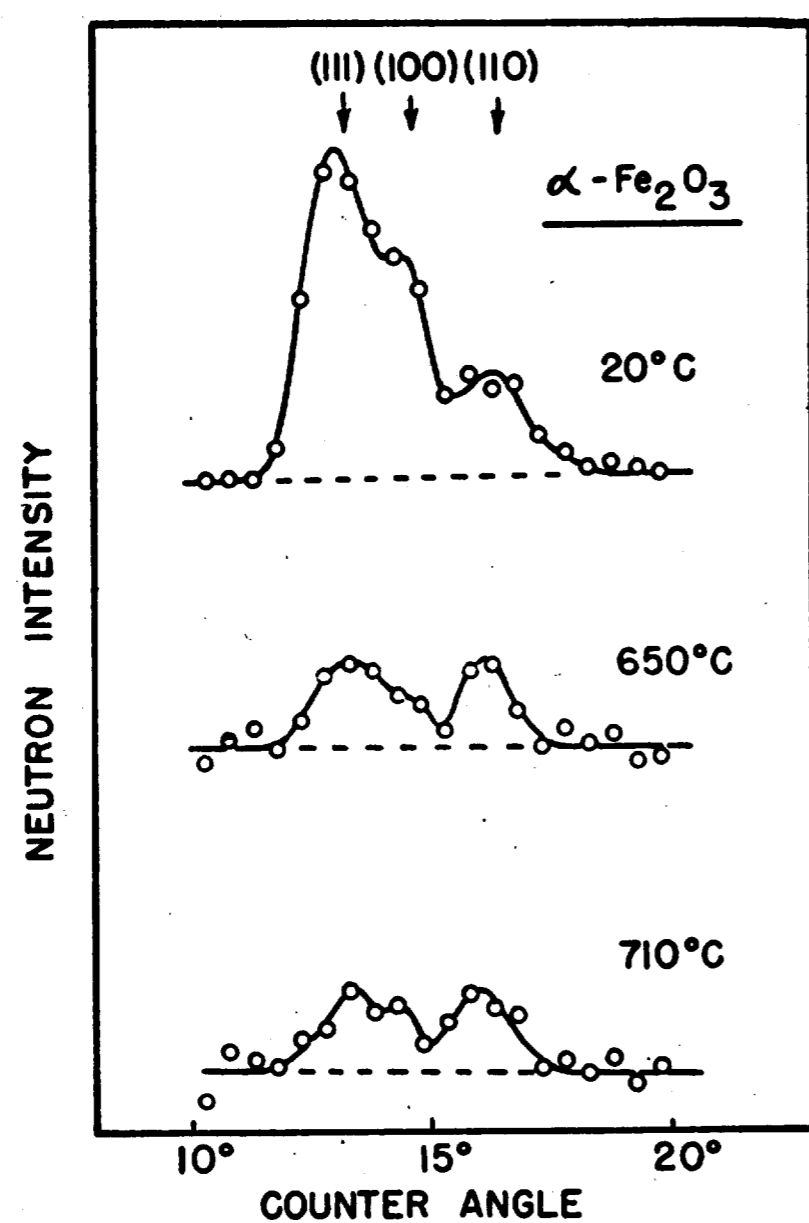

FIG. 14. Variation of α-Fe$_2$O$_3$ magnetic scattering intensity with temperature. The Curie temperature T_c is that obtained from magnetic susceptibility data.

STUDIES ON α-Fe$_2$O$_3$

The magnetic properties of α-Fe$_2$O$_3$ (hematite) have been studied by many observers, and widely different conclusions have been drawn concerning its magnetic structure. At room temperature very pure samples show weak ferromagnetic properties, which disappear at temperatures above 675°C. This Curie temperature is suspiciously close to that of Fe$_3$O$_4$ (magnetite), and Néel[28] considers that the observed ferromagnetism is parasitic and that the basic magnetic structure is that of an antiferromagnetic material. Very recently, Morin[29] has shown the room temperature ferromagnetism to disappear sharply at a temperature of $-20°C$, and below this the magnetic susceptibility can be accounted for on the basis of an antiferromagnetic lattice. Furthermore, Morin finds no crystallographic transition (by x-rays) above and below this low temperature transformation.

Neutron diffraction patterns have been taken for this substance over an extensive range, from 80°K to 1000°K, and these indicate the existence of an antiferromagnetic lattice throughout this temperature region but with some difference with temperature in structural detail. The room temperature pattern is shown in Fig. 12 along with an x-ray pattern for comparison purposes. All of the observed neutron reflections can be accounted for on the basis of permitted reflections for the chemical unit cell; therefore, the magnetic unit cell is suggested to be of the same size as the conventional chemical unit cell as determined by x-ray diffraction. This is a rhombohedral cell of edge length 5.42A and rhombohedral angle 55°17′, with two Fe$_2$O$_3$ molecules contained in the unit cell. The innermost two reflections (111) and (100) in Fig. 12 are the most interesting and informative in the neutron pattern. On the assumption that all Fe ions are alike in scattering power (justifiable for x-radi-

FIG. 13. Inner structure of α-Fe$_2$O$_3$ diffraction pattern at several temperatures. The (111) and (100) reflections are magnetic in origin and fall off at the higher temperatures, whereas the (110) is a nuclear reflection and is insensitive to temperature changes.

[26] J. H. Van Vleck, *Electric and Magnetic Susceptibilities* (Oxford University Press, London, 1932).

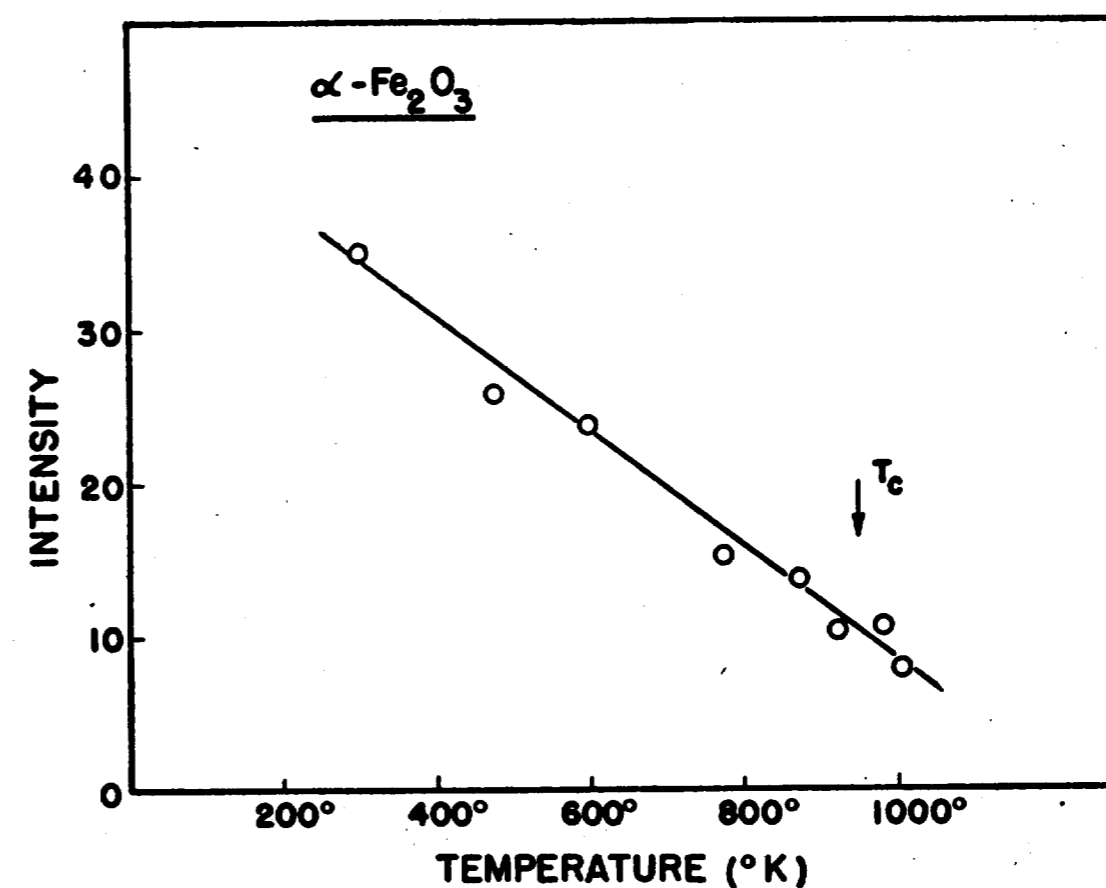[27] E. C. Stoner, *Magnetism and Matter* (Methuen and Company, Ltd., London, 1934).

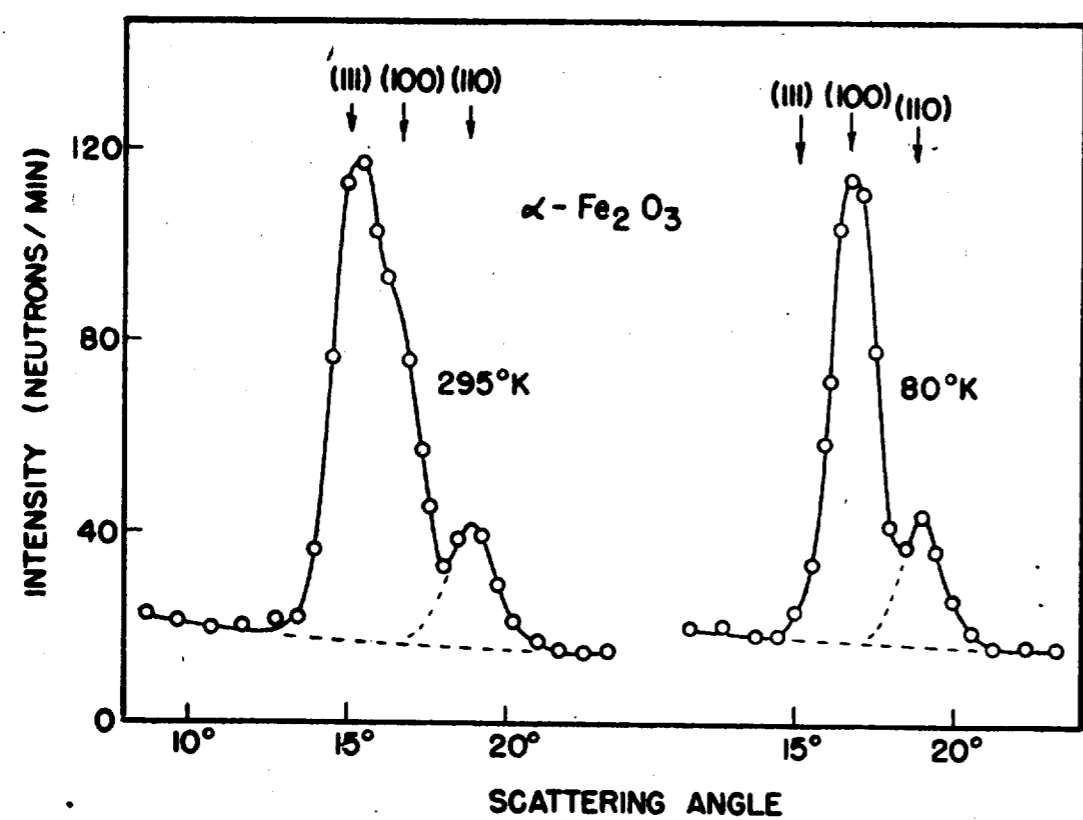[28] L. Néel, Ann. phys. 4, 249 (1949).

[29] F. J. Morin, Phys. Rev. 78, 819 (1950).

FIG. 15. Comparison of magnetic scattering in α-Fe$_2$O$_3$ at 295°K and 80°K. The magnetic intensities show a considerable rearrangement in cooling the sample below room temperature.

ation), there should be no scattered intensity in these reflections, because the crystal structure factors vanish in the summation over the unique atoms of the unit cell. There is pronounced neutron intensity at these positions, however, so that the magnetic orientation, or scattering power, must differ among the four Fe atoms of the unit cell.

Before discussing the magnetic structure of this material, it is desirable to present the temperature-dependent data which have been taken. The region of the diffraction pattern containing the (111), (100), and (110) reflections was studied at various elevated temperatures up to 730°C. The latter reflection is wholly nuclear in origin and should change only slightly due to the Debye-Waller temperature factor, whereas the other two magnetic reflections should exhibit characteristic Curie temperature behavior. Figure 13 shows typical curves at temperatures of 20°, 650°, and 710°C, and it is seen that the nuclear reflection remains essentially unchanged, whereas the magnetic reflections are sensitive to temperature changes. Figure 14 summarizes the magnetic intensity data, after correction for the Debye-Waller temperature factor as determined in the nuclear reflection, at various temperatures. The intensity variation is not nearly as pronounced as in the MnO case and, in fact, falls off with essentially a linear dependence on temperature. Even at the Curie temperature of 675°C, suspected from magnetic data, there
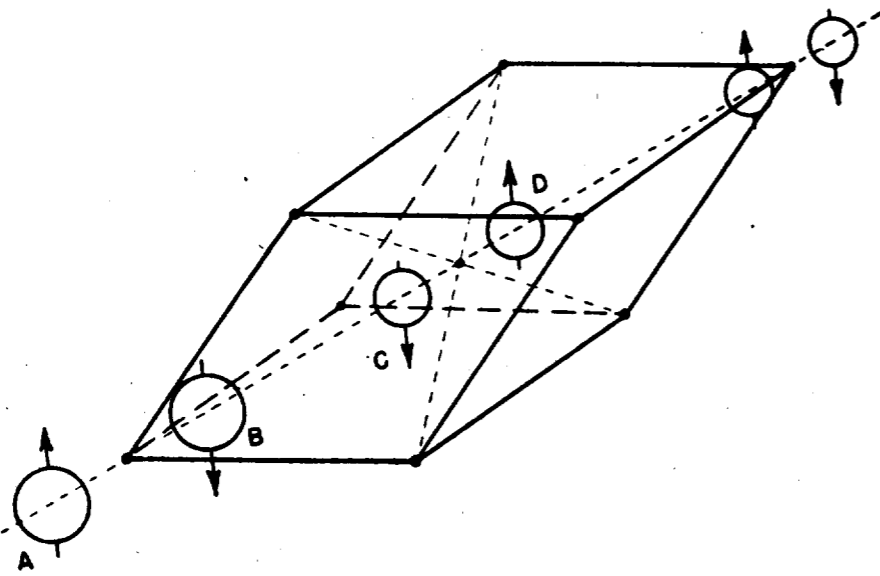

FIG. 16. Magnetic structure of α-Fe$_2$O$_3$ at room temperature. The rhombohedral unit cell containing four unique iron atoms is shown.

is still a remnance of the magnetic reflections. The patterns gave no indication of a reorganization of the structure, only a gradual fall-off in intensity.

In addition to the high temperature studies, the pattern at 80°K has been studied, and here a reorganization of the pattern appears. Figure 15 compares a portion of the 300°K and 80°K patterns, and it is seen that the normally strong (111) magnetic reflection has now become very weak or absent, whereas the (100) magnetic reflection has increased in intensity. The remaining reflections in the complete pattern showed little significant change; and these are not of much use in the structural arguments, because their weak intensity is not resolved from strong nuclear intensity. From observations on the pattern intensity when the sample was being cooled to low temperatures, it was established that the transformation occurred in the general vicinity of the −20°C transition, which had been found by Morin, although this was not studied in complete detail.

MAGNETIC STRUCTURE OF α-Fe$_2$O$_3$

As already mentioned, the neutron diffraction data suggest that the magnetic unit cell is the same size as

TABLE III. Comparison between observed and calculated F^2 values for various magnetic structure models of α-Fe$_2$O$_3$. The numbers are values calculated and observed for the differential scattering cross section F^2 in absolute units of 10^{-24} cm^2/Fe$_2$O$_3$ molecule.

| Case | Calculated for | | | | | | Observed | |
| (hkl) | Model (a) | | | Model (b) | | | 300°K | 80°K |
	(I)	(II)	(III)	(I)	(II)	(III)		
(111)	1.25	0	4.3	0.23	0	0.81	4.9	<0.05
(100)	1.40	1.59	0.96	2.32	2.64	1.59	0.91	1.37

the chemical unit cell and, hence, that there are four uniquely positioned Fe atoms in the cell, shown as ABCD in Fig. 16. There are three possible antiferromagnetic arrangements of relative spin orientation for these four atoms represented by Model (a) $+ - - +$, Model (b) $+ + - -$, and Model (c) $+ - + -$. Here Model (a) $+ - - +$ indicates that atoms A and D have parallel orientation (say, directed upward) while B and C both have antiparallel orientation (downward) with respect to that of A and D. Of these models, the crystal structure factors for Model (c) vanish in the (111) and (100) reflections, and hence, this model can be immediately excluded. Models (a) and (b) both predict finite intensities for these reflections, so it is to be hoped that the neutron data can show preference for one over the other. The observed intensities will depend not only upon the above model but also upon the orientation of the moments in the model with respect to the diffracting planes. For the absolute sense of orientation, the three most reasonable possibilities which have been considered are:

I. The moments are directed along the unit cell edges.

II. The moments are directed along the space diagonal of the unit cell and thus are perpendicular to the ferromagnetic (111) sheets in the lattice.

III. The moments are in the (111) sheets and directed towards one of the three nearest neighbors in the sheet.

Crystal structure factors have been calculated for these various cases using the magnetic scattering amplitude for Fe^{+++} given by Eq. (6) with $S=5/2$, there being 5 electrons in the $3d$-shell which contribute to the magnetic moment just as in the Mn^{++} ion. Table III summarizes these calculations for the (111) and (100) magnetic reflections for comparison with the observed values. All the values are given as differential scattering cross sections per Fe_2O_3 molecule, and both calculated and observed values are on an absolute scale. It is seen that the room temperature data suggest Model (a) with orientation III as being correct, while at low temperatures the suggested structure is that of Model (a) with orientation II. Thus, the low temperature data could be accounted for as simply a reorientation of the magnetic alignment from within the (111) sheets to one perpendicular to these sheets when the temperature is lowered.

The orientation results for the room temperature lattice fit in rather well with Néel's picture of the weak, parasitic ferromagnetism which is always observed. In his picture there exist small, distorted crystallites of magnetite intimately mixed with normal α-Fe_2O_3 layers in the layer structure built up along the trigonal axis perpendicular to the (111) sheets. In order to account for the directional properties of the weak ferromagnetism in single crystals of α-Fe_2O_3 observed by Smith[30] many years ago, Néel envisages the magnetic moment direction in the magnetite inclusions and in the α-Fe_2O_3 layers to be within the (111) sheets of the lattice. This is just the conclusion drawn from the neutron scattering observations.

The magnetic lattice for α-Fe_2O_3, shown in Fig. 16, exhibits characteristics similar to those of the magnetic lattice for the simple cubic oxides shown in Fig. 5. When additional unit cells to those shown in Fig. 16 are visualized, it is seen that the structure consists of a series of (111) sheets, within which all moments are arrayed ferromagnetically but with antiferromagnetic coupling between neighboring sheets. Interestingly, there are sheets of oxygen ions between each of the antiferromagnetically coupled sheets of iron ions. The alternating ferromagnetic sheet structure with intermediate oxygen planes was just that found in the cubic oxide magnetic structure.

[30] T. Townsend Smith, Phys. Rev. 8, 721 (1916).